

Irreversible Markov chains in spin models: Topological excitations

ZE LEI¹ (a) and WERNER KRAUTH^{1,2} (b)

¹ *Laboratoire de Physique Statistique, Département de physique de l'ENS, Ecole Normale Supérieure, PSL Research University, Université Paris Diderot, Sorbonne Paris Cité, Sorbonne Universités, UPMC Univ. Paris 06, CNRS, 75005 Paris, France*

² *Department of Physics, Graduate School of Science, The University of Tokyo, 7-3-1 Hongo, Bunkyo, Tokyo, Japan*

PACS 02.70.Tt – Justifications or modifications of Monte Carlo methods
PACS 75.10.Hk – Classical spin models
PACS 02.50.Ng – Distribution theory and Monte Carlo studies

Abstract – We analyze the convergence of the irreversible event-chain Monte Carlo algorithm for continuous spin models in the presence of topological excitations. In the two-dimensional XY model, we show that the local nature of the Markov-chain dynamics leads to slow decay of vortex–antivortex correlations while spin waves decorrelate very quickly. Using a Fréchet description of the maximum vortex–antivortex distance, we quantify the contributions of topological excitations to the equilibrium correlations, and show that they vary from a dynamical critical exponent $z \sim 2$ at the critical temperature to $z \sim 0$ in the limit of zero temperature. We confirm the event-chain algorithm's fast relaxation (corresponding to $z = 0$) of spin waves in the harmonic approximation to the XY model. Mixing times (describing the approach towards equilibrium from the least favorable initial state) however remain much larger than equilibrium correlation times at low temperatures. We also describe the respective influence of topological monopole–antimonopole excitations and of spin waves on the event-chain dynamics in the three-dimensional Heisenberg model.

Introduction. – Classical spin models have played a crucial role in the theory of critical phenomena and in the formulation of topological phases and their associated transitions. The analysis of vortices and their interactions in the two-dimensional XY model has lead, in particular, to the development of the Kosterlitz–Thouless theory [1], which initiated the era of topology in condensed-matter physics. Likewise, spin models have been instrumental in the continued development of the Markov-chain Monte Carlo method, and especially in the invention of advanced sampling methods. Cluster Monte Carlo algorithms [2] were of prime importance to show that Kosterlitz–Thouless theory actually applied to the phase transition in the two-dimensional XY-model [3]. Monte Carlo methods also elucidated the role of topological excitations in other models, such as the three-dimensional Heisenberg model [4].

In recent years, irreversible Monte Carlo algorithms have increasingly come into focus. In these methods, the asymptotic steady state (reached in the long-time limit)

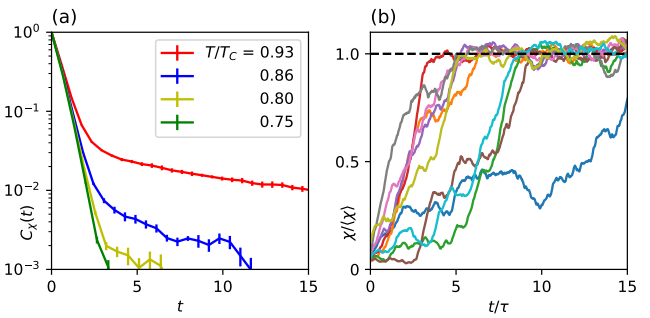


Fig. 1: Time evolution of the spin susceptibility in the XY model on a 64×64 square lattice (time t measured in sweeps). *Left:* Susceptibility autocorrelations below T_c . *Right:* Individual susceptibility evolutions at $T/T_c = 0.93$ starting from random initial configurations (equilibrium autocorrelation time τ). Large sample-to-sample fluctuations are apparent.

still corresponds to thermodynamic equilibrium, but it is realized with non-zero probability flows. The event-chain Monte Carlo algorithm [5,6], in particular, implements the

(a) ze.lei@ens.fr

(b) werner.krauth@ens.fr

global balance condition in a maximally asymmetric way. It relies on the concept of lifted Markov chains [7]. Besides short-range and long-range particle systems [8–10], the event-chain algorithm applies to continuous spin models such as the 2D and 3D XY model [11, 12] and the 3D Heisenberg model [13]. Improved convergence time scales were generally observed.

In this paper, we discuss the influence of topological excitations and of spin waves on the convergence of the event-chain algorithm, mostly concentrating on the two-dimensional XY model with its energy

$$E = -J \sum_{\langle i, j \rangle} \mathbf{S}_i \cdot \mathbf{S}_j, \quad (1)$$

with two-dimensional unit spins $\mathbf{S}_k = (S_k^x, S_k^y) = (\cos \phi_k, \sin \phi_k)$ on a square lattice with $N = L \times L$ sites. In eq. (1), the bracket \langle, \rangle denotes nearest neighbors. For the XY model, the event-chain algorithm (see [11]) rotates a given spin \mathbf{S}_i in positive sense in a sequence of infinitesimal moves until further rotation is vetoed through the factorized Metropolis algorithm [11]. At this event, spin i comes to a halt, and the neighbor that triggered the veto takes over, again rotating in positive direction. The event-chain algorithm violates the detailed-balance condition, but respects global balance. The latter is necessary to ensure convergence towards the equilibrium Boltzmann distribution. We also consider the harmonic approximation of the XY model [14], where in the energy of eq. (1) each term $\mathbf{S}_i \cdot \mathbf{S}_j = \cos(\phi_i - \phi_j)$ is approximated by $1 - \frac{1}{2}(\phi_i - \phi_j)^2$, and, finally, the three-dimensional Heisenberg model, where the spins \mathbf{S}_i are three-dimensional unit vectors. The XY model features vortex excitations and it is the unbinding of vortex–antivortex pairs which takes place at the critical temperature $T_c = 0.893J$. Below the critical temperature, however, the large-scale excitations of the XY model are spin waves. We will argue that the two-stage susceptibility autocorrelation at low temperature (see Fig. 1a) corresponds in fact to the fast decay of spin waves under event-chain dynamics and to the slow decay of the vortex–antivortex pairs. For $T/T_c \rightarrow 0$, where vortices are tightly bound, the event-chain algorithm is asymptotically fast ($z \approx 0$), as we corroborate by simulations. However, the equilibrium correlations do not give the complete picture of the time behavior of the Markov chain under consideration. Indeed, one may study the relaxation to equilibrium after a quench from another temperature (typically from $T = \infty$ to $T < T_c$). Here, a wide spectrum of relaxation times become relevant, and equilibration can take much longer than the equilibrium correlation time τ (see Fig. 1b). The quench dynamics is sensitive to the mixing time, which quantifies the approach towards equilibrium from the most unfavorable initial configuration [15]. Although the equilibrium correlations are described by a dynamical critical exponent $z \sim 0$ as $T/T_c \rightarrow 0$, we will argue that the mixing time remains at $z \sim 2$.

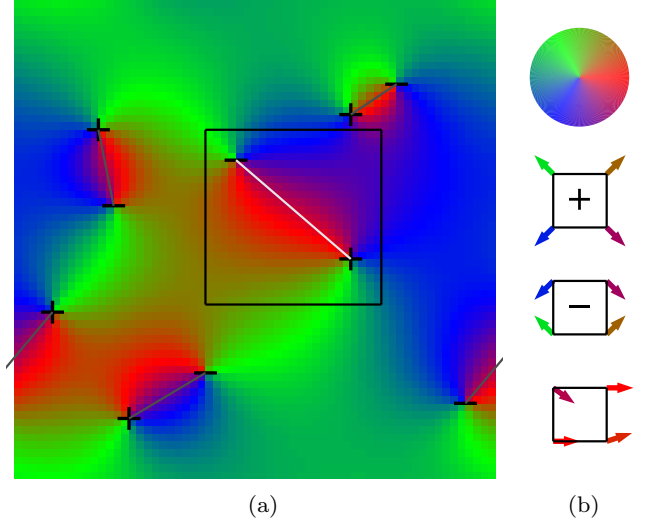


Fig. 2: Vortices in the XY model. *Left*: Configuration with 5 vortices (“+”) and 5 antivortices (“-”). The lines indicate matched vortex–antivortex pairs in the optimal assignment (see eq. (2)), and the length of the longest line (shown in white) equals the max-distance. A subsystem containing the max-distance pair is highlighted. *Right, from above*: Color code for the spin orientations, vortex, antivortex, and neutral plaquette configuration.

Vortex–antivortex pairs, max-distances. – For the XY model on a square lattice, vortices or antivortices, located on plaquettes delimited by four spins, are signalled by differences of neighboring spins that do not sum to zero when going around the plaquette in positive sense, but rather to 2π (vortex) or to -2π (antivortex) (see Fig. 2b). With periodic boundary conditions, vortices and antivortices appear in pairs. In a configuration with n such pairs, the vortices (v_1, v_2, \dots, v_n) can be paired up with the antivortices ($a_{P_1}, a_{P_2}, \dots, a_{P_n}$) according to one of the $n!$ permutations P . We suppose that the physically relevant pairing corresponds to the minimum of the Kosterlitz–Thouless vortex–antivortex-pair energy $\pi J_R \log(R) + 2E_c$, where the core energy E_c is the same for all configurations of n pairs and where the value of the renormalized stiffness J_R of Kosterlitz–Thouless theory does not influence the minimum [1]. We thus neglect interactions between different vortex–antivortex pairs. The proper association of each vortex v_i with its antivortex a_{P_i} defines an assignment problem (see Fig. 2a) aimed at minimizing the objective function ϵ :

$$\epsilon(\{v_i, a_{P_i}\}) = \sum_{i=1}^n \log |\mathbf{R}_{v_i} - \mathbf{R}_{a_{P_i}}|. \quad (2)$$

The optimal assignment of the n vortex–antivortex pairs can be determined with standard algorithms [16]. Among it, the pair (v_i, a_{P_i}) of largest separation defines the configuration’s *max-distance* d_{\max} . Remarkably, the time evolution of the max-distance during a computation mim-

ics that of the susceptibility (see Fig. 3). Large vortex–antivortex pairs (indicated by $d_{\max} \gg 1$) and small susceptibilities are particularly well correlated, and both persist on long time scales (see inset of Fig. 3).

We suggest that at low temperature the max-distance length scale determines the relaxation time scale. To show this, we prepare initial configurations with only two vortex pairs arranged in a square of length $d_{\max} = d$ (such a configuration can be constructed with periodic boundary conditions). We then track the time needed for the susceptibility to reach the equilibrium value (within a few percent). At temperature $T \sim T_c$, the system quickly generates many vortices that screen the distribution of the initial scale. In contrast, at low temperature, vortex–antivortex pairs at distance d must approach each other before they can be annihilated. Indeed, we find that the time to converge the square-shaped configuration of fixed d is independent of the system size L , and proportional to $\mathcal{O}(d^2)$. Taking $d = \mathcal{O}(L)$, this implies that the mixing time τ_{mix} (the time to reach equilibrium from the most unfavorable initial condition [15]), is at least $\mathcal{O}(L^2)$.

For $L \rightarrow \infty$, the probability to have a vortex–antivortex pair spaced by \mathbf{d} is:

$$\begin{aligned} P(\mathbf{d}) &= \frac{1}{Z} e^{-\beta E_p(d)} \\ &= \frac{1}{Z} (d)^{-\pi\beta J_R} \\ &\propto d^{-\pi\beta J_R}, \end{aligned} \quad (3)$$

where E_p is the pair energy of Kosterlitz–Thouless theory [1]. Because of eq. (3), the distribution of the max-distance for n vortices must be polynomial for $d_{\max} \rightarrow \infty$. For $T/T_c \rightarrow 0$, the power-law exponent must diverge as the vortex–antivortex pairs are more and more tightly bound.

Fréchet distribution, vortex max-distance. – At temperatures below T_c , for $L \rightarrow \infty$, vortex–antivortex pairs are bound [1], so that the equilibrium max-distance d_{\max} is much smaller than the system size, and its probability distribution $p(d_{\max})$ decays algebraically for large arguments (see eq. (3)). The $L \times L$ system can be divided into n^2 practically independent subsystems of size $L/n \times L/n$. The max-distance of the large system at scale L is the maximum of n^2 independent max-distances on a scale L/n . Extreme-value statistics [17] allows one to connect the distribution $p(d_{\max})$ at scale L with the one at L/n . It must correspond to the Fréchet distribution (with zero minimum value), specifically:

$$p(d_{\max}) = \frac{\alpha}{s} \left(\frac{d_{\max}}{s} \right)^{-1-\alpha} \exp \left[- \left(\frac{d_{\max}}{s} \right)^{-\alpha} \right] \quad (4)$$

with its cumulative distribution

$$P(d_{\max}) = \exp \left[- \left(\frac{d_{\max}}{s} \right)^{-\alpha} \right]. \quad (5)$$

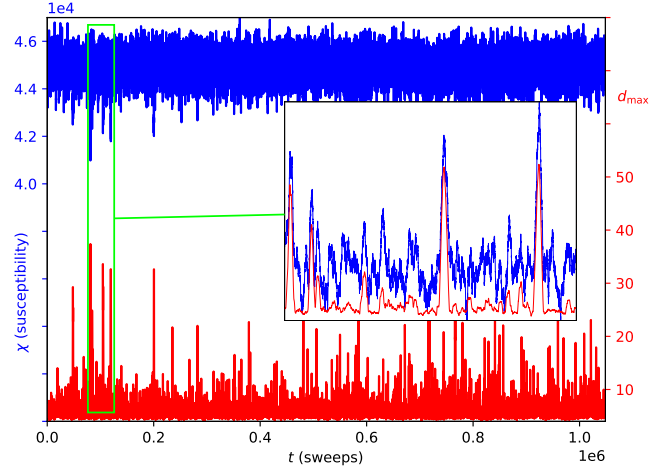


Fig. 3: Time-evolution of the vortex–antivortex max-distance in the 384×384 XY model at $T/T_c = 0.933$ compared to that of the susceptibility (smoothed over a small time window). The inset illustrates the correlation between max-distance and susceptibility in greater detail.

Here, α describes the power-law decay of the max-distance distribution for large arguments (which is the same on scales L and L/n), and s sets its L -dependent scale. The maximum of n independent samples of a Fréchet distribution with parameters (α, s) is distributed following a Fréchet distribution with parameters $(\alpha, n^{1/\alpha}s)$. It then follows that the Fréchet distribution of the max-distance in a system of size L must be described by parameters $(\alpha, L^{2/\alpha}s_0)$, where both α and s_0 depend on β , but not on L , for large L . Slightly below T_c already, the Fréchet distribution provides an excellent fit for the max-distance distribution and the fitting parameters α and s_0 are indeed independent of L for a given temperature (see Fig. 4). Also, we note that for $\alpha = 2$, the distribution of d_{\max} scales with $s \propto L$. This is observed for $T/T_c \rightarrow 1^-$. At low temperatures, we observe $\alpha \propto 1/T$, in agreement with eq. (3).

Below T_c , the probability distribution of d_{\max} scales as $\sim L^{2/\alpha} \ll L$, as $\alpha > 2$, and we expect the equilibrium correlation time to scale with $s^2 = L^{4/\alpha}s_0^2$:

$$\tau_{\text{corr}}^{\text{vortex}} \sim L^{4/\alpha} \sim \begin{cases} L^2 & \text{for } T \rightarrow T_c^- \\ L^{\text{const}T} & \text{for } T \rightarrow 0 \end{cases}. \quad (6)$$

The effective dynamical scaling parameter $z = 4/\alpha$ of the event-chain algorithm is thus connected to the scale parameter of a Fréchet distribution and predicted to vanish in the zero-temperature limit.

Harmonic model, spin waves. – The ansatz of eq. (6) for the equilibrium correlations only describes the relaxation of topological excitations, parametrized by the max-distance. We now consider spin waves which, below T_c , are the dominant large-distance excitations for local

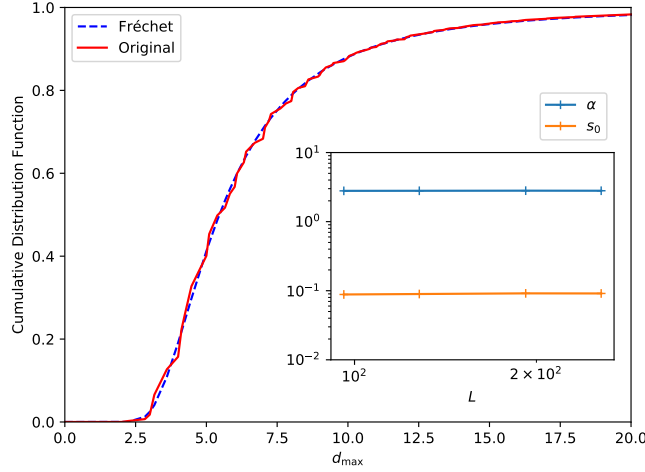


Fig. 4: Cumulative max-distance distribution in the XY model at $L = 256$ and $T/T_c = 0.965$ fitted with the Fréchet distribution with $\alpha = 2.80$ and $s = 4.79$ ($s_0 = 0.0913$). The inset illustrates that the fitting parameters α and s_0 are independent of L .

Monte Carlo dynamics, where they take $\mathcal{O}(L^2)$ sweeps to relax. In the event-chain algorithm, they relax in $\mathcal{O}(L^0)$ sweeps, so that our ansatz is indeed consistent. To show this, we study the harmonic model, an approximation to the XY Hamiltonian, where the spin variables ϕ interact as follows:

$$E = \frac{J}{2} \sum_{\langle i,j \rangle} (\phi_i - \phi_j)^2. \quad (7)$$

This model is exactly solved by taking Fourier modes as the independent variables [14]. The two-dimensional harmonic model has algebraically decaying spin correlations with an exponent that approaches zero as $T/T_c \rightarrow 0$. From the exact solution of the harmonic model, it follows that the difference of ϕ on sites distant by $\mathcal{O}(L)$ is on a scale

$$\sigma^{\text{eq}}(L) \propto \begin{cases} \sqrt{L} & \text{if } d = 1 \\ \sqrt{\log L} & \text{if } d = 2 \\ 1 & \text{if } d \geq 3 \end{cases}.$$

The event-chain algorithm for the harmonic model can only increase the value of ϕ_i . We find that in one sweep ($\mathcal{O}(N)$ events), the mean value $\langle \phi_i \rangle$ of a configuration increases by $\mathcal{O}(1)$. The correlation time of the algorithm is reached when the mean increase per site is on the order of the equilibrium correlation σ^{eq} . This implies the relation

$$\tau_{\text{corr}}^{\text{harm}} \sim \sigma^{\text{eq}}(L). \quad (8)$$

The eq. (8) predicts a dynamical scaling exponent of $1/2$ for the 1D harmonic model, and an exponent $z = 0$ in higher dimensions. This fast dynamical scaling, in sharp contrast to the behavior of the local Metropolis algorithm (with $z \sim 2$) is verified for the autocorrelation times for Fourier modes with small \mathbf{k} (see Fig. 5).

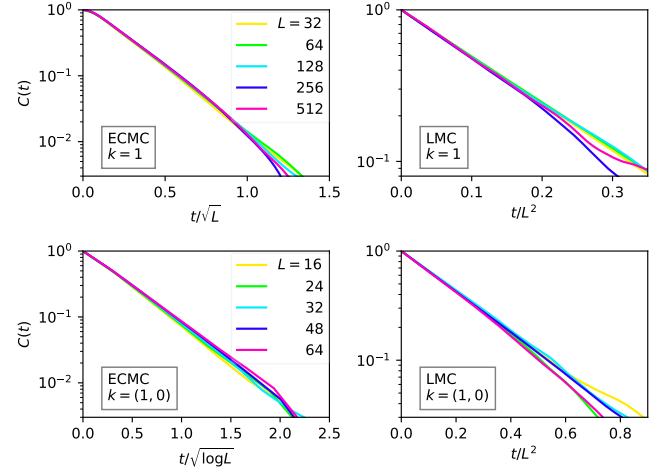


Fig. 5: Equilibrium auto-correlation functions $C(t)$ of the lowest Fourier modes in the harmonic model for the event-chain algorithm (ECMC) and for local Monte Carlo (LMC). *Upper*: $C(t)$ for the Fourier mode $k = 1$ in 1D. *Lower*: $C(t)$ for the Fourier mode $k = (1, 0)$ in 2D. Data are in agreement with the scaling of eq. (8).

In the XY model below T_c , the two types of excitations generate two time scales for the equilibrium autocorrelation function of the event-chain algorithm. This corresponds to what is observed in the susceptibility, where we thus associate the fast initial decay with spin waves ($\tau_{\text{corr}}^{\text{harm}} \sim \text{const}$), and the slow decay with topological excitations (vortex-antivortex pairs, $\tau_{\text{corr}}^{\text{vortex}} \sim L^{\text{const}T}$ at low temperature and $\tau_{\text{corr}}^{\text{vortex}} \sim L^2$ for $T/T_c \rightarrow 1^-$) (see Fig. 1).

Monopoles, Bloch waves. — Topological excitations also play a prominent role in other spin models, for example the 3D Heisenberg model. Low-temperature excitations in that model can also be described by spin waves in addition to topological excitations. Spin waves again come with a dynamical critical exponent ~ 0 . Heisenberg-model monopoles and anti-monopoles are again located on the dual lattice, and they can be identified using a well-defined algorithm [18].

In the 3D Heisenberg model, monopole-antimonopole pairs proliferate near the critical point [4]. Their excitation energy increases with the separation d as $\mathcal{O}(d)$ [19, 20]. The event-chain algorithm, at low temperature, again moves each monopole or antimonopole by $\mathcal{O}(1)$ per sweep. From initial configurations with pairs separated on a scale $\mathcal{O}(L)$, we find that relaxation towards equilibrium takes $\mathcal{O}(L)$ sweeps (rather than $\mathcal{O}(L^2)$, as for the XY model). Configurations with widely separated pairs play no role at low temperature, and the spin waves are again treated efficiently in the event-chain algorithm, so that $z \rightarrow 0$ for $T/T_c \rightarrow 0$. Nevertheless, the mixing time scale for the approach to equilibrium from an unfavorable configuration is $\mathcal{O}(L)$ sweeps.

Finally, there are other types of topological excitations,

besides the point-like ones (vortices, monopoles) discussed here. Bloch modes, in the XY model with periodic boundary conditions, correspond for example to a state in which the spins rotate by 2π as one coordinate, say x , goes from 0 to L . Bloch waves are a slow mode in the event-chain algorithm for the XY model (but not in the Heisenberg model), and stable on a time scale $\mathcal{O}(L^2)$ at low temperature in both 2D and 3D.

Conclusions. — In this paper, we exhibited a considerable speed-up for the relaxation of spin-wave excitations of the event-chain algorithm compared to the local Monte Carlo algorithm. Indeed, in the harmonic model, which has only spin waves, the event-chain algorithm equilibrates in a constant number of sweeps for $d > 1$, whereas the local algorithm equilibrates with $z \sim 2$. We have also studied the relaxation of topological excitations, namely the vortex–antivortex pairs in the 2D XY model and the monopole–antimonopole pairs in the Heisenberg model. In the XY model, below the critical temperature, vortex–antivortex pairs are bound, and we parametrize this binding with a single parameter, the max-distance d_{\max} that can be computed with a combinatorial-optimization algorithm. We find that the probability distribution of d_{\max} is a Fréchet distribution (with zero minimum value). In the XY model, the vortex–antivortex potential is very weak, leading to a d_{\max}^2 relaxation time and, at worst, an L^2 mixing time. However, equilibrium-correlation time scales are much smaller. In the event-chain algorithm, these vortex–antivortex excitations are no longer concealed by the spin waves, and they in fact constitute the slowest dynamical modes for the event-chain algorithm. It is thus found to have a smaller dynamical exponent than the local Monte Carlo algorithm for all temperatures below T_c . In particle systems, we likewise expect the fast relaxation of phonon modes (which, in analogy to the spin waves of this paper, are also described by a harmonic model) to be key to the success of the event-chain algorithm at high densities [8]. However, the fundamental difference between mixing times (needed to reach equilibrium from the most unfavorable initial condition) and equilibrium correlation times (needed to move to a new independent configuration from an equilibrium starting configuration) appears clearly [15]. It will certainly have to be taken into account in applications.

We thank Youjin Deng for helpful discussions in the initial stages of this work and Cris Moore for useful suggestions.

REFERENCES

- [1] KOSTERLITZ J. M. and THOULESS D. J., *J. Phys. C*, **6** (1973) 1181.
- [2] WOLFF U., *Phys. Rev. Lett.*, **62** (1989) 361.

- [3] HASENBUSCH M., *J. Phys. A*, **38** (2005) 5869.
- [4] HOLM C. and JANKE W., *J. Phys. A*, **27** (1994) 2553.
- [5] BERNARD E. P., KRAUTH W. and WILSON D. B., *Phys. Rev. E*, **80** (2009) 056704.
- [6] MICHEL M., KAPFER S. C. and KRAUTH W., *J. Chem. Phys.*, **140** (2014) 054116.
- [7] DIACONIS P., HOLMES S. and NEAL R. M., *Ann. Appl. Probab.*, **10** (2000) 726.
- [8] BERNARD E. P. and KRAUTH W., *Phys. Rev. Lett.*, **107** (2011) 155704.
- [9] KAPFER S. C. and KRAUTH W., *Phys. Rev. Lett.*, **114** (2015) 035702.
- [10] HARLAND J., MICHEL M., KAMPMANN T. A. and KIERFELD J., *EPL*, **117** (2017) 30001.
- [11] MICHEL M., MAYER J. and KRAUTH W., *EPL*, **112** (2015) 20003.
- [12] KIMURA K. and HIGUCHI S., arXiv:1709.01665 (2017).
- [13] NISHIKAWA Y., MICHEL M., KRAUTH W. and HUKUSHIMA K., *Phys. Rev. E*, **92** (2015) 063306.
- [14] WEGNER F., *Z. Phys.*, **206** (1967) 465.
- [15] LEVIN D. A., PERES Y. and WILMER E. L., *Markov Chains and Mixing Times* (American Mathematical Society) 2008.
- [16] PAPADIMITRIOU C. H. and STEIGLITZ K., *Combinatorial Optimization: Algorithms and Complexity* (Prentice-Hall) 1982.
- [17] DE HAAN, L. and FERREIRA A., *Extreme Value Theory: An Introduction* (Springer Science & Business Media) 2007.
- [18] BERG B. and LÜSCHER M., *Nucl. Phys. B*, **190** (1981) 412.
- [19] LAU M. and DASGUPTA C., *J. Phys. A*, **21** (1988) L51.
- [20] OSTLUND S., *Phys. Rev. B*, **24** (1981) 485.